Monolithic Finite Element Method for the simulation of thixo-viscoplastic flows

N. Begum[*], **A. Ouazzi**[†], **S. Turek**[‡]

Institute for Applied Mathematics, LS III, TU Dortmund University, D-44227 Dortmund, Germany
[*]Naheed.Begum@math.tu-dortmund.de; [†]Abderrahim.Ouazzi@math.tu-dortmund.de; [‡]ture@featflow.de

Key words: Thixo-viscoplastic Flows, FEM, Newton-Multigrid, Monolithic, Generalized Navier-Stokes equations, Incompressible fluids

Abstract: This note is concerned with the application of Finite Element Method (FEM) and Newton-Multigrid solver to simulate thixo-viscoplastic flows. The thixo-viscoplastic stress dependent on material microstructure is incorporated via viscosity approach into generalized Navier-Stokes equations. The full system of equations is solved in a monolithic framework based on Newton-Multigrid FEM Solver. The developed solver is used to analyze the thixo-viscoplastic flow problem in a Lid-driven cavity configuration.

1 INTRODUCTION

The thixo-viscoplastic flows are introduced into yield stress flows by taking in consideration the internal material micro-structure using a structure parameter λ. Firstly, the viscoplastic stress is modified to include the thixotropic stress dependent on the structure parameter

$$\begin{cases} \sigma(\lambda) = 2\eta(\lambda)\mathbf{D}(u) + \tau(\lambda)\dfrac{\mathbf{D}(u)}{\|\mathbf{D}(u)\|}, & \text{if } \|\mathbf{D}(u)\| \neq 0, \\ \|\sigma(\lambda)\| \leq \tau(\lambda), & \text{if } \|\mathbf{D}(u)\| = 0, \end{cases} \tag{1}$$

where $\mathbf{D}(u)$ denotes the strain rate tensor. The norm for a tensor Λ is given by $\|\Lambda\| = \sqrt{\mathrm{Tr}(\Lambda^2)}$. We use $\|\mathbf{D}(u)\|$ and $\|\mathbf{D}\|$ alternately. η denotes plastic viscosity, and τ defines a yield stress that is a threshold parameter from which the material starts yielding. The shear stress has two contributions: a viscous part, and a strain rate independent part. Secondly, an evolution equation for the structure parameter is introduced to induce the time-dependent process of competition between the destruction (breakdown) and the construction (buildup) inhabited in the material

$$\left(\frac{\partial}{\partial t} + u \cdot \nabla\right)\lambda = \mathcal{F} - \mathcal{G}, \tag{2}$$

where, $\mathcal{F}$ and $\mathcal{G}$ are two nonlinear functions representing the buildup and breakdown of material micro-structure. A collection of thixotropic models with various choices of η, τ, $\mathcal{F}$ and $\mathcal{G}$ is given in Table 1;

Table 1: Thixotropic models

	η	τ	$\mathcal{F}$	$\mathcal{G}$
Worrall & Tulliani [16]	$\lambda\eta_0$	τ_0	$a(1-\lambda)\|\mathbf{D}\|$	$b\lambda\|\mathbf{D}\|$
Coussot et al.[4]	$\lambda^g\eta_0$		a	$b\lambda\|\mathbf{D}\|$
Houška [6]	$(\eta_0+\eta_1\lambda)\|\mathbf{D}\|^{n-1}$	$(\tau_0+\tau_1\lambda)$	$a(1-\lambda)$	$b\lambda^m\|\mathbf{D}\|$
Mujumbar et al. [9]	$(\eta_0+\eta_1\lambda)\|\mathbf{D}\|^{n-1}$	$\lambda^{g+1}G_0\Lambda_c$	$a(1-\lambda)$	$b\lambda\|\mathbf{D}\|$
Dullaert & Mewis [3]	$\lambda\eta_0$	$\lambda G_0(\lambda\|\mathbf{D}\|)\Lambda_c$	$(a_1+a_2\|\mathbf{D}\|)(1-\lambda)t^p$	$b\lambda\|\mathbf{D}\|t^{-p}$

where η_0 and τ_0 are initial plastic viscosity and yield stress resp. in the absence of any thixotropic phenomena, η_1 and τ_1 are thixotropic plastic viscosity and yield stress. Λ_c is the critical elastic strain,

https://doi.org/10.4995/YIC2021.2021.12250

and G_0 is the elastic modulus of unyielded material. a and b are buildup and breakage constants, and g, p, m, n are rate indices.

In quasi-Newtonian modeling approach for thixo-viscoplastic flows, an extended viscosity $\mu(\cdot,\cdot)$ is used for the generalized Navier-Stokes equations [10]. As for instance [13]:

$$\mu(D_{II},\lambda) = \eta(D_{II},\lambda) + \tau(D_{II},\lambda)\frac{\sqrt{2}}{2}\frac{1}{\sqrt{D_{II}}}\left(1 - e^{-k\sqrt{D_{II}}}\right), \tag{3}$$

where k is the regularization parameter. The generalized Navier-Stokes equations and the evolution equation for the structure parameter constitute the full set of modeling equations which is given as follows:

$$\begin{cases} \left(\dfrac{\partial}{\partial t} + u\cdot\nabla\right)u - \nabla\cdot\Big(2\mu(D_{II},\lambda)\mathbf{D}(u)\Big) + \nabla p = 0, & \text{in } \Omega, \\ \nabla\cdot u = 0, & \text{in } \Omega, \\ \left(\dfrac{\partial}{\partial t} + u\cdot\nabla\right)\lambda - \mathcal{F}(D_{II},\lambda) + \mathcal{G}(D_{II},\lambda) = 0, & \text{in } \Omega, \end{cases} \tag{4}$$

where u denotes velocity, p the pressure, λ the structure parameter, $\mathcal{F}$ and $\mathcal{G}$ the nonlinear functions for buildup and breakdown of material micro-structure. $D_{II} = \frac{1}{2}\big(\mathbf{D}(u) : \mathbf{D}(u)\big)$ is the second invariant of the strain rate tensor $\mathbf{D}(u)$.

2 FINITE ELEMENT DISCRETIZATION

To derive the variational form for thixo-viscoplastic flows, we consider the spaces $\mathbb{T} := L^2(\Omega), \mathbb{V} := (H_0^1(\Omega))^2$, and $\mathbb{Q} := L_0^2(\Omega)$ associated, respectively, with the corresponding L^2-norm, $\|\cdot\|_0$, H^1-norm, $\|\cdot\|_1$, and L^2-norm, $\|\cdot\|_0$. Let $\tilde{u} := (\lambda, u, p) \in \big(\mathbb{T}\cap H^1(\Omega)\big)\times\mathbb{V}\times\mathbb{Q}$, and $\tilde{v} := (\xi, v, q) \in \mathbb{T}\times\mathbb{V}\times\mathbb{Q}$ be a test function. The weak formulation for the thixo-viscoplastic flows reads: *Find* $\tilde{u} \in \big(\mathbb{T}\cap H^1(\Omega)\big)\times\mathbb{V}\times\mathbb{Q}$ *s. t.*

$$a_\lambda(\tilde{u})(\lambda,\xi) + a_u(\tilde{u})(u,v) + b(v,p) - b(u,q) = 0, \quad \forall\tilde{v}\in\mathbb{T}\times\mathbb{V}\times\mathbb{Q}, \tag{5}$$

where $a_\lambda(\tilde{u})(\cdot,\cdot)$, $a_u(\tilde{u})(\cdot,\cdot)$, and $b(\cdot,\cdot)$ are given as follows

$$a_\lambda(\tilde{u})(\lambda,\xi) = \int_\Omega \Big(-\mathcal{F}(D_{II},\lambda) + \mathcal{G}(D_{II},\lambda)\Big)\xi\, d\Omega + \int_\Omega u\cdot\nabla\lambda\,\xi\, d\Omega, \tag{6}$$

$$a_u(\tilde{u})(u,v) = \int_\Omega 2\mu(D_{II},\lambda)\mathbf{D}(u) : \mathbf{D}(v)\, d\Omega + \int_\Omega u\cdot\nabla u\, v\, d\Omega, \tag{7}$$

$$b(v,q) = -\int_\Omega \nabla\cdot v\, q\, d\Omega. \tag{8}$$

The finite element approximations of the problem (5) have to take care of its saddle point character, due to the bilinear form (8). Furthermore, since thixo-viscoplastic flows are usually slow, the only remaining issue is the control/continuity of the bilinear form (6) in the norm of space $\mathbb{T}$. We opt for higher order stable pair bi-quadratic for velocity and piece-wise linear discontinuous for the pressure, Q_2/P_1^{disc}, and higher order quadratic for structure parameter Q_2 with the appropriate stabilization terms [10, 15]. Indeed, let the domain Ω be partitioned by a grid $K \in \mathcal{T}_h$ which are assumed to be open quadrilaterals such that $\Omega = \text{int}\big(\bigcup_{k\in\mathcal{T}_h}\overline{K}\big)$. For an element $K \in \mathcal{T}_h$, we denote by $\mathcal{E}(K)$ the set of all 1-dimensional edges of K. Let $\mathcal{E}_i := \bigcup_{k\in\mathcal{T}_h}\mathcal{E}(K)$ be the set of all interior element edges of the grid $\mathcal{T}_h$.

We define the conforming finite element spaces $\mathbb{T}_h \subset \mathbb{T}$, $\mathbb{V}_h \subset \mathbb{V}$, and $\mathbb{Q} \subset \mathbb{Q}_h$ such that:

$$\mathbb{T}_h = \Big\{\xi_h \in \mathbb{T}, \xi_{h|K} \in\ Q_2(K)\,\forall\, K\in\mathcal{T}_h\Big\}, \tag{9}$$

$$\mathbb{V}_h = \big\{v_h \in \mathbb{V}, v_{h|K} \in\ (Q_2(K))^2\,\forall\, K\in\mathcal{T}_h,\, v_h = 0 \text{ on } \partial\Omega_h\big\}, \tag{10}$$

$$\mathbb{Q}_h = \Big\{q_h \in \mathbb{Q}, q_{h|K} \in\ P_1^{\text{disc}}(K)\,\forall\, K\in\mathcal{T}_h\Big\}. \tag{11}$$

The approximate problem reads: *Find* $\tilde{u} \in \mathbb{T}_h \times \mathbb{V}_h \times \mathbb{Q}_h$ *s. t.*

$$a_\lambda(\tilde{u})(\lambda,\xi) + j_{\tilde{u}}(\tilde{u},\tilde{v}) + a_u(\tilde{u})(u,v) + b(v,p) - b(u,q) = 0, \quad \forall \tilde{v} \in \mathbb{T}_h \times \mathbb{V}_h \times \mathbb{Q}_h. \tag{12}$$

The stabilization term $j_{\tilde{u}}(\cdot,\cdot)$ is given as follows

$$j(\cdot,\cdot) := j_u(\cdot,\cdot) + j_\lambda(\cdot,\cdot), \tag{13}$$

$$j_u(u,v) = \sum_{E\in\mathcal{E}_i} \gamma_u |E|^2 \int_E [\nabla u]\,[\nabla v]\, d\sigma, \tag{14}$$

$$j_\lambda(\lambda,\xi) = \sum_{E\in\mathcal{E}_i} \gamma_\lambda |E|^2 \int_E [\nabla \lambda]\,[\nabla \xi]\, d\sigma. \tag{15}$$

The stabilization (13) is consistent, control the convective terms and makes the coercivity and continuity match in $\mathbb{T}_h$ associated with the norm $|||\cdot|||$, where

$$|||\xi|||^2 = \|\xi\|_0^2 + j_\lambda(\xi,\xi). \tag{16}$$

3 GENERALIZED DISCRETE NEWTON

We use the Newton method to approximate the nonlinear residuals. Let $\mathcal{R}(\tilde{u}) = (\mathcal{R}_\lambda(\tilde{u}), \mathcal{R}_u(\tilde{u}), \mathcal{R}_p(\tilde{u})) = \big(\mathcal{R}_{(\lambda,u)}(\tilde{u}), \mathcal{R}_p(\tilde{u})\big)$ denote the residuals for the system (12). The nonlinear iteration is updated with the correction $\delta\tilde{u}$, $\tilde{u}^{k+1} = \tilde{u}^k + \delta\tilde{u}$. Then, the Newton linearization gives the following approximation for the residuals:

$$\mathcal{R}(\tilde{u}^{l+1}) = \mathcal{R}(\tilde{u}^l + \delta\tilde{u}) \simeq \mathcal{R}(\tilde{u}^l) + \left[\frac{\partial \mathcal{R}(\tilde{u}^l)}{\partial \tilde{u}}\right] \delta\tilde{u}. \tag{17}$$

The Newton's method iterations, assuming invertible Jacobians, are given as follows:

$$\tilde{u}^{l+1} = \tilde{u}^l - \omega_l \left[\frac{\partial \mathcal{R}(\tilde{u}^l)}{\partial \tilde{u}}\right]^{-1} \mathcal{R}(\tilde{u}^l). \tag{18}$$

The damping parameter $\omega_l \in (0,1)$ is chosen such that

$$\left\|\mathcal{R}(\tilde{u}^{l+1})\right\| \leq \left\|\mathcal{R}(\tilde{u}^l)\right\|. \tag{19}$$

The damping parameter is not sufficient for the convergence of this type of highly nonlinear problem, mainly due to the presence of Jacobian's singularities related to the problem or simply by being out of the domain of Newton's convergence [8, 10]. We use a generalized Newton's method which consists of using approximate Jacobians far away from the quadratic convergence range or close to singularities and accurate Jacobians in the quadratic region of convergence in an adaptive way [8]. Indeed, based on a priori analysis of Jacobians property. Let the Jacobian be written as follows:

$$\left(\frac{\partial \mathcal{R}(\tilde{u}^l)}{\partial \tilde{u}}\right) = \left(\frac{\partial \tilde{\mathcal{R}}(\tilde{u}^l)}{\partial \tilde{u}}\right) + \delta_l \left(\frac{\partial \hat{\mathcal{R}}(\tilde{u}^l)}{\partial \tilde{u}}\right). \tag{20}$$

The Jacobian (20) is splitted into a direct sum of corresponding operators with different properties. The parameter $\delta_l \in (0,1)$ is solely dependent on the rate of actual residual convergence [8]. It is worth mentioning that the operator-related damped Jacobian method (20) is related to the continuous Newton's method. The Jacobian approximation is only dependent on the rate of the actual residual convergence $\left(\left\|\mathcal{R}^l\right\| / \left\|\mathcal{R}^{l-1}\right\|\right)$. This generalized Newton's method assures a global nonlinear convergence [8].

4 MONOLITHIC MULTIGRID LINEAR SOLVER

To develop an appropriate linear solver, we segregate the Jacobian as follows

$$\left(\frac{\partial \mathcal{R}(\tilde{u})}{\partial \tilde{u}}\right) = \begin{pmatrix} \dfrac{\partial \mathcal{R}_{(\lambda,u)}(\tilde{u})}{\partial(\lambda,u)} & \dfrac{\partial \mathcal{R}_u(\tilde{u})}{\partial p} \\ \dfrac{\partial \mathcal{R}_p(\tilde{u})}{\partial u} & 0 \end{pmatrix}, \tag{21}$$

which is a saddle point problem. Then, the resulting linear system is treated with a Multilevel Pressure Schur Complement (MPSC) approach with Vanka-like smoother i.e.

$$\tilde{u}^{k+1} = \tilde{u}^k - \omega_k \sum_{K \in \mathcal{T}_h} \left(\left(\frac{\partial \mathcal{R}(\tilde{u}^l)}{\partial \tilde{u}} \right)_{|K} \right)^{-1} \mathcal{R}(\tilde{u}^l)_{|K}. \tag{22}$$

In (22), we solve exactly on real element, K, and perform an outer Gau-Seidel iteration [5]. We use standard geometric multigrid solver for linearized system with standard Q_2 and P_1^{disc} restriction and prolongation operators. The combination of a stable finite element approximations, Q_2/P_1^{disc}, for Stokes problem together with multigrid results in a high numerically accurate, flexible, and efficient FEM-multigrid solver.

5 THIXO-VISCOPLASTIC FLOW IN LID-DRIVEN CAVITY

Lid-driven cavity flows represent an academic common standard benchmark for incompressible CFD codes. Therefore, we present the corresponding results for Newtonian, viscoplastic, and thixo-viscoplastic flows. Furthermore, this problem is accepted as a test configuration to check points wise mesh convergences despite the lack of regularity due to the pressure singularity in the corners of upper-lid. From thixotropic collection models given in Table 1, we use Houška's material model ($m = 1$).

5.1 Newtonian flow in lid-driven cavity

The global accuracy of the approximation which consist of the L_2-norm of the velocity is investigated using the kinetic energy. On the other hand, the point wise accuracy is investigated using the velocity magnitude at vertical center-line beside the primary vortex and the lower left secondary vortex. In order to check the solver convergence, we list in Table 2 the kinetic energy, $\frac{1}{2}\int_\Omega \|u\|^2\, dx$, and Newton-multigrid iterations, the number of nonlinear iteration versus the average number of multigrid sweeps (N/M), w.r.t. mesh refinement for an increased Reynolds numbers $Re = 1000$, $Re = 5\,000$, and $Re = 10\,000$. The starting solution for any level is the interpolated one from one level coarser. Table 3 shows the primary vortex and lower left secondary vortex w.r.t. mesh refinement for Reynolds numbers $Re = 1000$, $Re = 5\,000$, and $Re = 10\,000$. Moreover, we provide in Figure 1 the stream function contours for the mesh refinement level 9 and the velocity magnitude at vertical center-line w.r.t. mesh refinement for Reynolds numbers $Re = 1000$, $Re = 5\,000$, and $Re = 10\,000$.
As can be seen in Table 2, grid independent results are achieved for the kinetic energy, as well as for Newton-multigrid solver. It is worth mentioning that for the coarser levels few extra nonlinear iterations are required in contrast to finer mesh due to the decrease of interpolation error in the starting solutions.

Table 2: **Newtonian flow in lid-driven cavity**: The kinetic energy and the number of Newton-multigrid iterations, nonlinear number of iterations and the average number of multigrid iterations (N/M), for different mesh refinement at Reynolds numbers $Re = 1\,000$, $Re = 5\,000$, and $Re = 10\,000$.

Re		1 000		5 000		10 000	
Level	cells	Energy$\times 10^2$	N/M	Energy$\times 10^2$	N/M	Energy$\times 10^2$	N/M
7	16384	4.452357	3/1	4.768669	4/1	4.868399	5/1
8	65536	4.451904	3/1	4.744815	3/2	4.783917	4/2
9	262144	4.451846	3/1	4.742921	3/1	4.773500	3/2
10	1048576	4.451834	2/1	4.742815	3/1	4.772692	3/1
Ref. values $\approx$		4.45		4.74		4.77	

Table 3: **Newtonian flow in lid-driven cavity**: The primary vortex and the lower left secondary vortex at $Re = 1\,000$, $Re = 5\,000$, and $Re = 10\,000$.

Re	1000		5000		10000	
Level	ψ_{max}	$\psi_{min} \times 10^3$	ψ_{max}	$\psi_{min} \times 10^3$	ψ_{max}	$\psi_{min} \times 10^3$
7	0.1189360	-1.72649	0.1225439	-3.077555	0.1236127	-3.2070181
8	0.1189361	-1.72851	0.1222499	-3.072411	0.1225210	-3.1831353
9	0.1189362	-1.72963	0.1222269	-3.073524	0.1224097	-3.1910101
10	0.1189366	-1.72965	0.1222259	-3.073589	0.1223892	-3.1797390
Ref.	0.1189[1]	-1.729[1]	0.1221[7]	-3.070[1]		

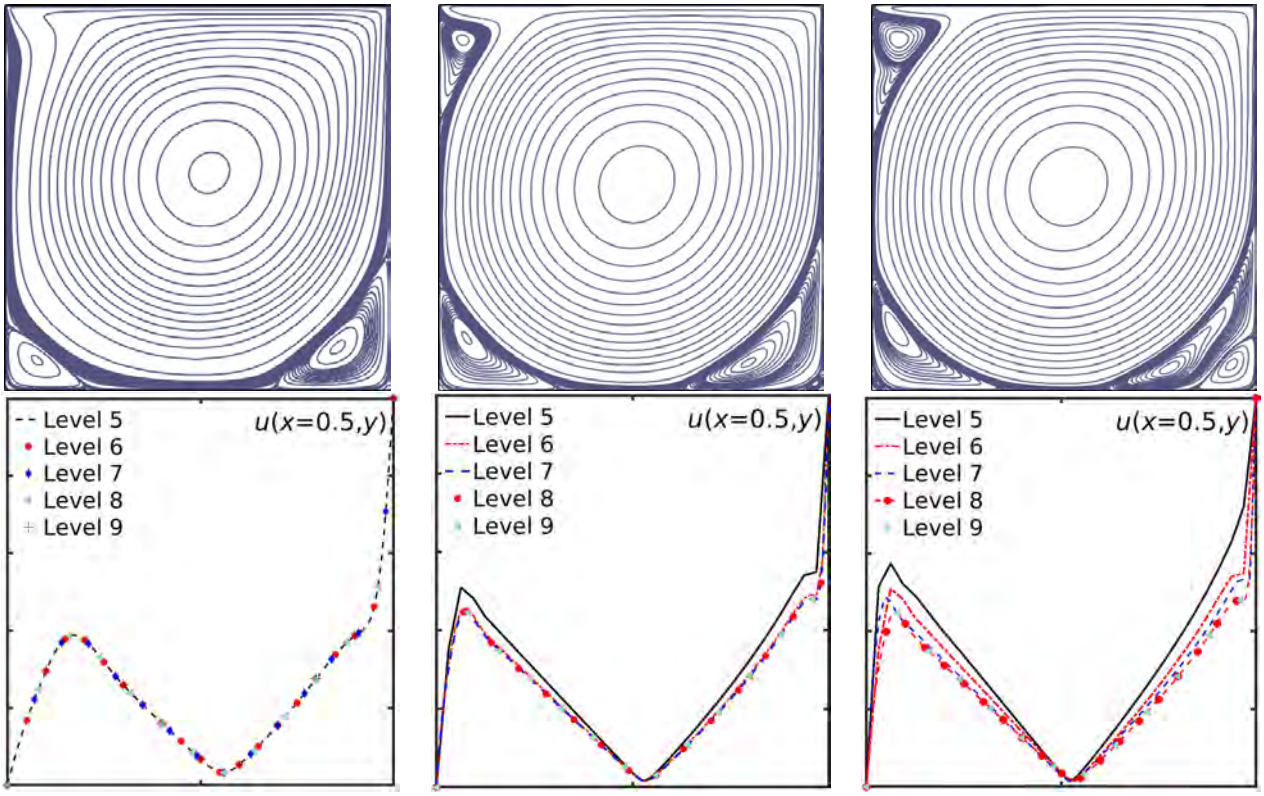

Figure 1: **Newtonian flow in lid-driven cavity:** The stream-function's contours at mesh refinement level 9 (TOP) and velocity magnitude at vertical centerline w.r.t. mesh refinement (BOTTOM) computed for Reynolds numbers $Re = 1\,000$, $Re = 5\,000$, and $Re = 10\,000$ resp. (LEFT to RIGHT).

5.2 Viscoplastic flow in lid-driven cavity flow

We acheived point wise convergence under mesh refinement for Newtonian flow. Moreover, no further improvement by increasing the resolution beyond mesh refinement level 8. Now, we investigate the impact of the regularization parameter in quasi-Newtonian modeling approach for viscoplastic flow. Figure 2 shows the boundary limit of the numerical approximation of the rigid zone w.r.t. regularization parameter k. Clearly, the relative convergence of the boundary limit of the rigid zone w.r.t. regularization parameter k is obtained. Furthermore, there is an optimal regularization $K_L \approx 2^{L8} \approx 10^3$ from from which there is no further accuracy improvement in capturing the rigid zone by increasing the regularization parameter k. In Figure 3, we use the optimal choice of the regularization parameter

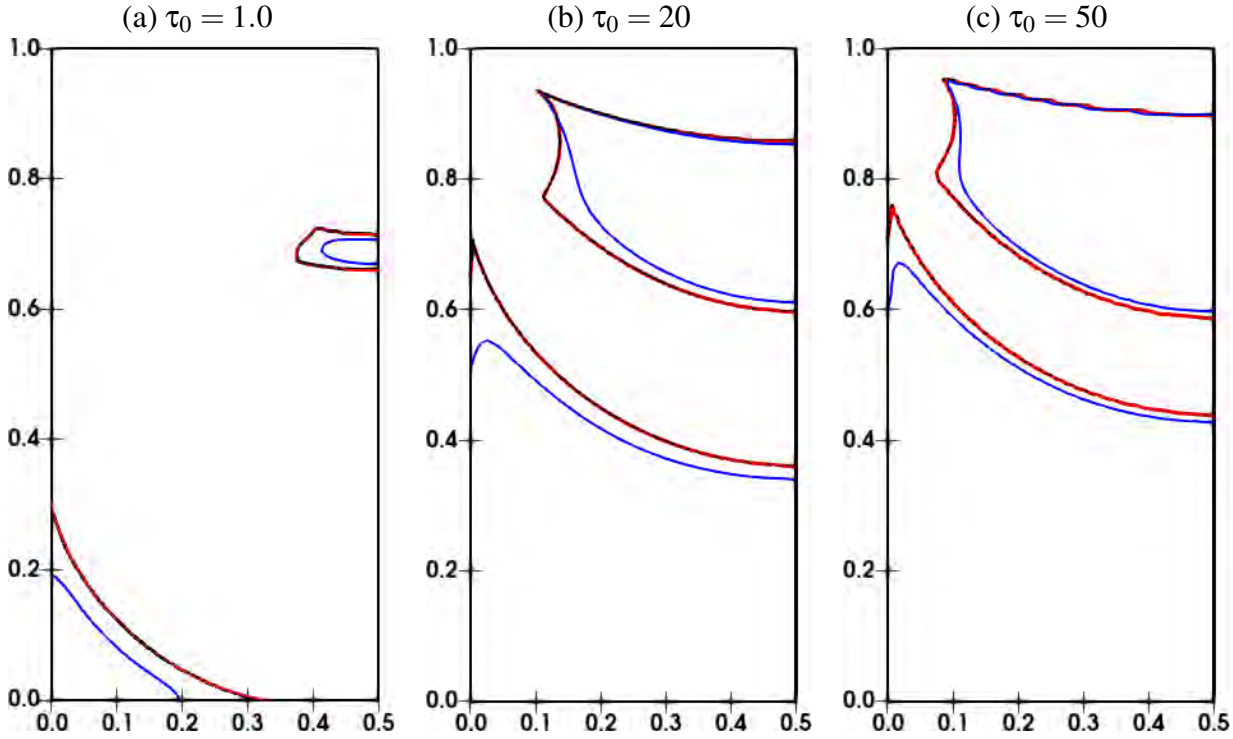

Figure 2: **Non-thixotropic (Bingham plastic) flow in lid-driven cavity:** The boundary limit of the numerical approximation of the plastic/rigid zone w.r.t. regularization parameter k, $k = 10^2$ (blue), $k = 10^3$ (red) and $k = 10^4$ (black), for different non-thixotropic yield stress parameter τ_0. The other parameters are set to $\eta_0 = 1.0$, $\eta_1 = 0.0$, and $\tau_1 = 0.0$. The solutions are calculated at mesh-refinement level 8.

and mesh refinement level to predict the relative position of the rigid zone to stream function contours for an increased non-thixotropic yield stress parameter $\tau_0 = 1$, $\tau_0 = 2$, $\tau_0 = 5$, $\tau_0 = 10$, $\tau_0 = 20$, and $\tau_0 = 50$. Furthermore, we provide the corresponding Newton-multigid data in Table 4 which depicts the number of Newton-multigrid iterations, i.e. the nonlinear number of iterations and the average number of multigrid iterations (N/M), w.r.t. different regularization parameters k and mesh refinement levels L. The solutions are calculated using the continuations process w.r.t. regularization k.
From Table 4, we conclude the Newton-multigrid solver is mesh refinement independent. Clearly, the nonlinearity of the problem is increased by increasing the non-thixotropic yield stress parameter τ_0, But, the slightly increases in the nonlinearity w.r.t. mesh refinement is due to the continuation process w.r.t. regularization parameter k used to obtain the solutions.

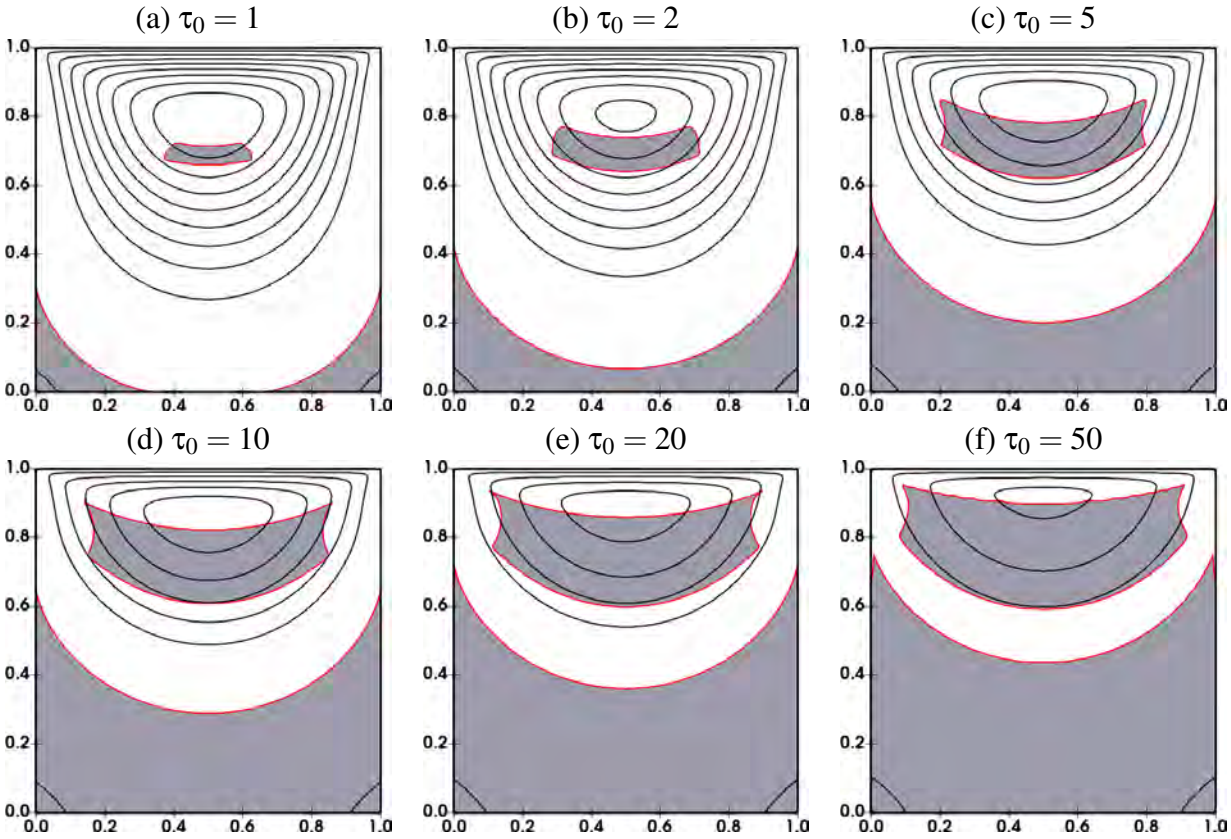

Figure 3: **Non-thixotropic (Bingham plastic) flow in lid-driven cavity:** The relative position of the plastic/rigid zone to streamline contours for an increased non-thixotropic yield stress parameter τ_0. The other parameters are set to $\eta_0 = 1.0$, $\eta_1 = 0.0$, and $\tau_1 = 0.0$. The Papanastasiou regularization parameter is set to $k = 10^4$. The solutions are calculated at mesh-refinement level 8.

Table 4: **Non-thixotropic (Bingham plastic) flow in lid-driven cavity**: The number of Newton-multigrid iterations, nonlinear number of iterations and the average number of multigrid iterations (N/M), w.r.t. different regularization parameters k and mesh refinement levels L for Bingham viscoplastic flow for different values of non-thixotropic yield stress parameters τ_0.

$k\backslash L$	5	6	7	5	6	7	5	6	7
	$\tau_0 = 1$			$\tau_0 = 2$			$\tau_0 = 5$		
1×10^1	3/1	3/1	3/1	3/1	3/1	3/1	4/1	4/1	4/1
1×10^2	3/1	3/1	3/1	3/1	3/1	3/1	4/1	4/1	4/1
1×10^3	2/2	3/2	3/1	3/1	3/1	4/1	4/1	5/2	5/2
1×10^4	2/1	2/2	5/1	3/1	3/1	6/1	4/1	5/4	6/3
	$\tau_0 = 10$			$\tau_0 = 20$			$\tau_0 = 50$		
1×10^1	5/1	5/1	5/1	6/1	6/1	6/1	5/1	7/1	7/1
1×10^2	5/2	4/1	4/1	5/2	5/2	5/1	6/5	5/4	5/1
1×10^3	5/2	7/4	9/1	5/5	7/2	8/1	5/5	9/2	9/2
1×10^4	6/1	7/2	8/3	6/3	5/5	7/3	6/3	7/3	8/2

5.3 Thixo-viscoplastic flow in lid-driven cavity flow

Armed with the knowledge of the point wise mesh convergence of viscoplastic driven cavity flow. Indeed, we obtained the point wise convergence of the boundary limit of the rigid zone w.r.t. the regularization parameter k. Furthermore, there is pair $(K,L) \approx (2^{L8},L8)$ regularization and mesh refinement level beyond which no further resolution improvement is possible. Now, we are ready the investigate thixo-viscoplastic driven cavity. Figure 4 sets out the relative position of the rigid zone to stream function contours for an increased thixotropic yield stress parameter τ_1. The solutions are calculated with the resolution barrier pair (K,L).

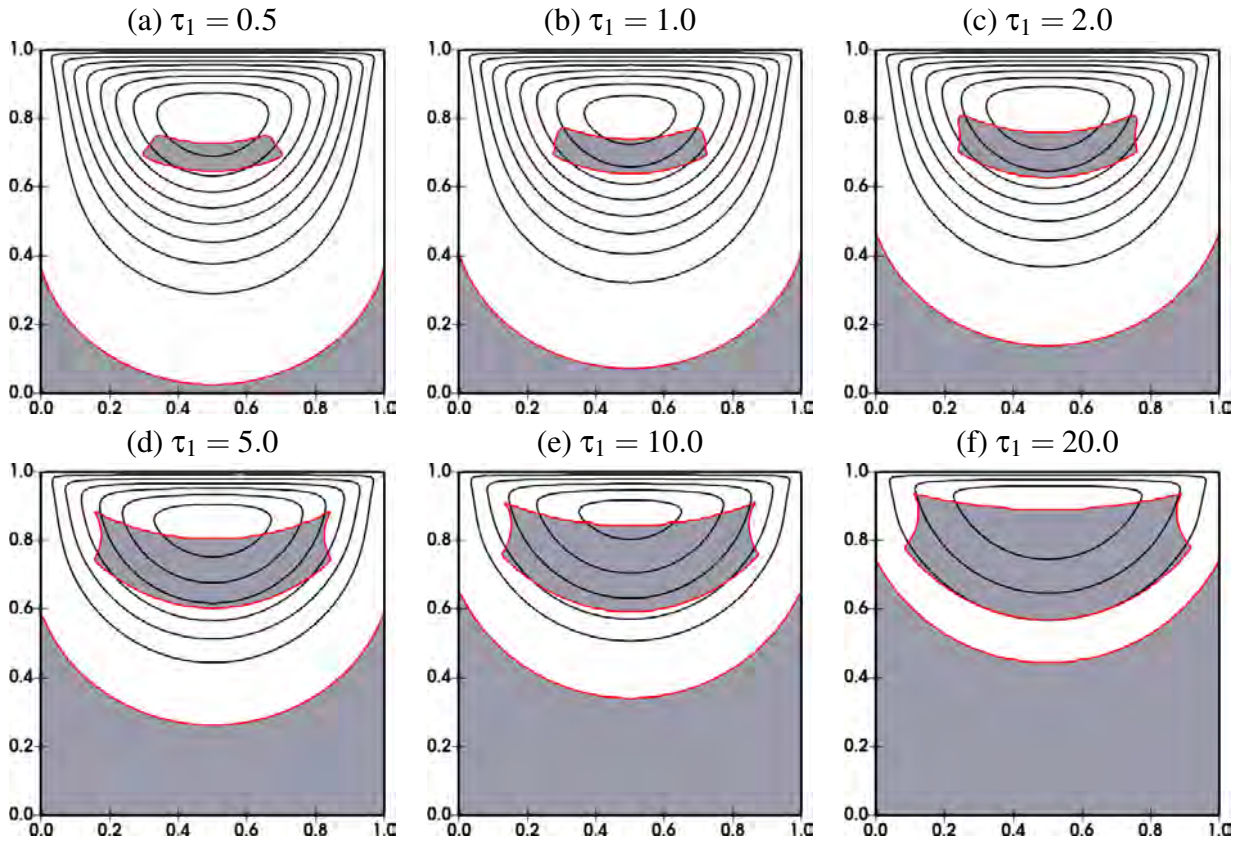

Figure 4: **Thixo-viscoplastic flow in lid-driven cavity:** The relative position of the plastic/rigid zone to streamline contours for an increased thixotropic yield stress parameter τ_1. The other parameters are set to $\eta_0 = 1.0$, $\eta_1 = 0.0$, $\tau_0 = 1.0$, $a = 1.0$ and $b = 0.1$. The Papanastasiou regularization parameter is set to $k = 10^4$. The solutions are calculated at mesh-refinement level 8.

In Table 5, we summarize the number of Newton-multigrid iterations, nonlinear number of iterations and the average number of multigrid iterations (N/M), w.r.t. different regularization parameters k and mesh refinement levels L for thixo-viscoplastic flow for different values of thixotropic yield stress parameters τ_1. The solutions are calculated using the continuations process w.r.t. regularization k.

Table 5 shows the mesh refinement independent of Newton-multigrid solver. Indeed, the nonlinearity of the problem is increased by increasing the thixotropic yield stress parameter τ_1, But, the slightly increases in the nonlinearity w.r.t. mesh refinement is due to the continuation process w.r.t. regularization parameter k used to obtain the solutions.

Table 5: **Thixo-viscoplastic flow in lid-driven cavity**: The number of Newton-multigrid iterations, nonlinear number of iterations and the average number of multigrid iterations (N/M), w.r.t. different regularization parameters k and mesh refinement levels L for thixo-viscoplastic flow for different values of thixotropic yield stress parameters τ_1. The solutions are calculated using the continuations process w.r.t. regularization k.

$k\backslash L$	5	6	7	5	6	7	5	6	7
	$\tau_1 = 0.5$			$\tau_1 = 1$			$\tau_1 = 2$		
1×10^1	5/2	5/3	6/2	5/2	5/2	9/1	5/2	5/2	9/1
1×10^2	4/1	4/2	5/1	4/1	4/2	7/1	4/2	4/2	8/1
1×10^3	4/1	4/1	4/1	4/2	4/2	8/1	4/4	6/1	7/1
1×10^4	4/1	4/2	4/2	5/1	7/1	4/1	7/1	10/1	8/2
	$\tau_1 = 5.0$			$\tau_1 = 10.0$			$\tau_1 = 20.0$		
1×10^1	6/2	6/2	10/1	11/1	8/2	11/1	10/1	9/2	11/1
1×10^2	4/2	5/2	11/1	10/1	5/3	8/1	12/1	6/3	10/1
1×10^3	5/2	9/1	10/1	10/1	9/1	7/1	8/2	9/1	9/2
1×10^4	5/1	5/2	5/1	8/3	7/1	5/1	8/2	7/1	9/1

6 SUMMARY

We presented a Newton-multigrid FEM solver for the quasi-Newtonian modeling approach for thixotropic flows. Based on a two-fields Stokes solver, we used higher order stable Q_2/P_1^{disc} FE approximations for velocity and pressure and higher order Q_2 FE approximation for the structure parameter field with appropriate stabilization term. The combination of a stable finite element approximations, Q_2/P_1^{disc}, for Stokes problem together with multigrid results in high numerically accurate, flexible and efficient FEM-multigrid solver. The nonlinearity is handled with generalized Newton's method w.r.t. the Jacobian's singularities having a global convergence property. For the numerical investigations; we used lid-driven cavity benchmark to find out the optimal setting, mesh refinement, and regularization. Indeed, we achieved a point-wise mesh convergence as well as a resolution barrier, (k,L) regularization mesh refinement level, beyond which no further resolution's improvement is possible. Furthermore, the solver shows a mesh refinement independency. For viscoplastic and thixo-viscoplastic solutions, we used the discrete continuation process w.r.t. regularization which might be integrated continuously within the solver in a black box manner.

Acknowledgments: The authors acknowledge the funding provided by the Deutsche Forschungsgemeinschaft (DFG, German Research Foundation) - 446888252. Additionally, the authors acknowledge the financial grant provided by the Bundesministerium fr Wirtschaft und Energie aufgrund eines Beschlusses des Deutschen Bundestages through AiF-Forschungsvereinigung: Forschungs- Gesellschaft Verfahrens Technik e. V. - GVT under the IGF project number 20871 N. We would also like to gratefully acknowledge the support by LSIII and LiDO3 team at ITMC, TU Dortmund University, Germany.

REFERENCES

[1] Bruneau, C., Saad, M., The 2D lid-driven cavity problem revisited.*Computers & Fluids* (2006) **35**:326–348.

[2] Burgos, G. R., Alexandrou, A. N., Entov, V. Thixotropic rheology of semisolid metal suspensions. *J. Mater. Process. Technol.* (2001) **110**(2):164–176.

[3] Dullaert, K., Mewis, J. A Structural kinetics model for thixotropy. *J. Non-Newton. Fluid Mech.* (2006) **139**:21–30.

[4] Coussot, P., Nguyen, Q. D., Huynh, H. T., Bonn, D. Viscosity bifurcation in thixotropic, yielding fluids. *J. Rheol.* (2002) **46**(3):573–589.

[5] Damanik, H., Hron, J., Ouazzi, A., Turek, S. A monolithic FEM–multigrid solver for non–isothermal incompressible flow on general meshes. *J. Comp. Phys.* (2009) **228**:3869–3881.

[6] Houška, M. *Engineering aspects of the rheology of thixotropic liquids*. PhD thesis, Faculty of Mechanical Engineering, Czech Technical University of Prague, (1981).

[7] Kupperman, R. A central-difference scheme for a pure stream function formulation of incompressible viscous flow. *SIAM J. Sci. Comp.* (2001) **23**.

[8] Mandal, S., Ouazzi, A., Turek, S. Modified Newton solver for yield stress fluids, *Proceedings of ENUMATH 2015, the 11th European Conference on Numerical Mathematics and Advanced Applications*, Springer, (2016):481-490.

[9] Mujumdar, A., Beris, A. N., Metzner, A. B. Transient phenomena in thixotropic systems. *J. Nonnewton. Fluid Mech.* (2002) **102**(2):157–178.

[10] Ouazzi, A. *Finite Element Simulation of Nonlinear Fluids. Application to Granular Material and Powder*, Shaker Verlag, Achen (2006).

[11] Begum, N., Ouazzi, A., Turek, S. Monolithic Newton-multigrid FEM for the simulation of thixotropic flow problems.*Ergebnisberichte des Instituts fr Angewandte Mathematik Nummer 638, Fakultt fr Mathematik*, TU Dortmund University 634, (2021).

[12] Ouazzi, A., Begum, N., Turek, S. Newton-multigrid FEM solver for the simulation of quasi-newtonian modeling of thixotropic flows.*Ergebnisberichte des Instituts fr Angewandte Mathematik Nummer 638, Fakultt fr Mathematik*, TU Dortmund University 638, (2021).

[13] Papanastasiuo, T.C., Flow of materials with yield. *J. Rheol.*, (1987) **31**:385-404.

[14] Moller, P., Fall, A., Chikkadi, V. and Derks, D. and Bonn, D, An attempt to categorize yield stress fluid behaviour. *Phil Trans. R. Soc. A*, (2009) **367**:5139-5155.

[15] Turek, S., Ouazzi, A. Unified edge–oriented stabilization of nonconforming FEM for incompressible flow problems: Numerical investigations. *J. Numer. Math.* (2007) **15**(4):299–322.

[16] Worrall, W. E., Tuliani, S. Viscosity changes during the aging of clay-water suspensions. *Trans. Brit. Ceramic Soc.* (1964) **63**:167-185.